THERMAL RADIATION PROPERTIES OF CERIA-THORIA MANTLE FABRIC

D. M. Mason

Institute of Gas Technology
Chicago, Illinois 60616

Introduction

Gas lighting has been based on the Welsbach mantle since its introduction in the 1890's, and little new scientific information on its operation or on that of other forms of flame-heated thermal light radiators has appeared since 1918. However, during the last 20 years new burner technology has emerged; porous plate and surface combustion burners for production of infrared radiation are particularly noteworthy. In many applications where radiant heating is effective there is an accompanying need for lighting. Potential applications include patios, restaurants, stadiums, warehouses, and foundaries. At the time this work was undertaken it appeared that development of combination lighting and heating devices could fill a real need. The investigation reported here was undertaken to obtain information that would allow us to design, or at least guide the development of, new light and heat radiating devices.

Previous Studies of Emittance of Ceria-Thoria

Rubens investigated the Welsbach mantle, composed of thoria and ceria (1). He found that the mantle, when hot, had a high emittance in the blue region of the visible spectrum. By optical pyrometry in this wavelength region, with corrections obtained from reflectance measurements, he estimated its temperature to be about 1550°C. He found the high efficiency of the 99% thoria, 1% ceria mixture to be due to two causes: first, to the low emittance of the thoria, particularly in the near infrared, by virtue of which it attains a high temperature in the flame; second, to a high emittance in the visible region imparted by the presence of ceria. He showed that thoria alone has too little emittance in the visible range to give much light, while ceria, in amounts greater than about 1%, increased the emittance in the near infrared, lowering the temperature and the emission in the visible range. This is because blackbody radiation at the relevant temperatures occurs mainly in the near infrared, and secondly because in the visible range the intensity of blackbody radiation varies by a much higher power of the absolute temperature than does the total radiation.

Ives, Kingsbury, and Karrer in 1918 published an extensive investigation of mantle materials (2). Alumina, beryllia, magnesia, silica, and zirconia were investigated as base materials in comparison with thoria. Uranium, manganese, nickel, lanthanum, praseodymium, neodymium, and erbium were investigated as colorants, but none of these were superior to cernium. Temperatures of mantles prepared from the various base materials were determined by measurements with thermocouples of different wire sizes, so that results could be extrapolated to zero wire diameter. The spectral emittance of the oxides were also measured. These measurements confirmed the theory that thoria has less total emittance in the infrared than other refractory

oxides, although it is not lowest in the 1 to 5μm region. Magnesia was next best. Ives et al. concluded that if higher temperatures should become feasible, then wavelengths beyond 5μm would have relatively less effect on the radiation and magnesia would become as good as, or better than, thoria.

In agreement with Rubens' observations, the emittance of thoria was found to increase as the concentration of ceria was increased. The increase was uniform and gradual in the infrared, while in the visible, and particularly in the blue, the increase was very abrupt. As pointed out by Rubens, the ordinary mantle with approximately 1% of ceria is practically black (emits and absorbs like a blackbody) in the blue end of the spectrum when it is hot. This behavior, in contrast to the whiteness of the cold mantle, is ascribed to the occurrence of an absorption-emission band of the ceria in the near ultraviolet, which broadens into the visible at elevated temperatures. The yellow color of the ordinary mantle that is observed as the mantle cools after the fuel is turned off is caused by this absorption band.

Ives et al. also found that the effect of the ceria on visible radiation was highly dependent on the oxidizing-reducing conditions (2). When the flame is adjusted so that the mantle is in the reducing part of the flame, the emittance became much less selective; that is, emittance in the blue decreased and emittance elsewhere increased. Mantle fabric heated in the reducing part of the flame and cooled without access to air come out dark gray, but if reheated in an oxidizing flame, regained its ordinary color. Similar results were obtained when the mantle was heated in hydrogen or in a cathode discharge tube.

Ritzow and other investigators made emittance measurements on bulk ceria-thoria and found higher emittance in the near infrared than Ives or Rubens obtained on mantles (3). (The consolidated state of the material and the greater thickness of the section probably caused the increase in emittance from <0.02 to about 0.20.) With bulk material Ritzow found a decrease in emittance with the addition of ceria, then an increase with addition of greater amounts (4). Liebman made measurements on pure thoria in the visible (5). Similar measurements in the infrared were made at the National Bureau of Standards over the range 1200° to 1600°K.

The emittance of a material is related to its intrinsic absorption coefficient. The coefficient of thorium oxide was determined at room temperature in the visible by Weinrich (6), from measurements on fused thoria. He showed that the color of thoria changes from red to colorless when it is heated in a vacuum at 1000°C and can be changed back to red by reheating it in air at the same temperature. A change in absorption spectrum accompanies the treatments. A different spectrum again is obtained after heating the thoria to 1800°C under vacuum. He attributed these effects to changes in oxygen content and defect structure. A small but measurable change in weight was observed with the 1800°C treatment but not with the 1000°C treatment.

Alumina is the only oxide whose intrinsic absorption coefficient, from 0.5 to 6μm, has been determined at elevated temperatures (7). According to these measurements temperature has a much greater effect on the absorption coefficient at shorter wavelengths (1 to 3μm) than at longer wavelengths. Emittance determinations at the National Bureau of Standards confirm this observation not only for alumina but also for thoria, magnesia, and zirconia (8).

Theory of Radiation Characteristics of Translucent Materials

Thermal emission is usually thought of as a surface effect. This is a good approximation for metals, where absorption and emission occur within 1 wavelength of the surface. However, with dielectrics — which, when not too thick, are usually transparent or translucent — not only the surface but also the volume of the material is involved. Because radiation is emitted from and penetrates into the bulk of the material, it is necessary to consider transmission and scattering of the radiation as well as surface absorption and emission.

Development of Kubelka-Munk Equations

One method of treating this problem is by the Kubelka-Munk theory, which was first developed for media under conditions where emission need not be considered. In this form, the theory has been applied to many problems, such as the transmission of light through fog, reflection and transmission of light by opal glass, and reflection by paint, paper, and plastics. The theory was extended by Hamaker to include emission from the medium (9).

According to this theory, we consider a slab or sheet of an isotropic nonhomogeneous (light-scattering) dielectric. Its lateral extent is large compared with the distance required for opacity, and its thickness and other conditions, including external illumination (if any), are taken to be uniform from point to point in the lateral plane. Radiation in the material is diffuse; that is, it occurs in every direction, although not necessarily uniformly so. We consider the radiation to be composed of two parts, one traveling inward from one face of the slab and the other outward. These fluxes are labeled I and J as indicated by the arrows in Figure 1. It is understood that I is composed of the hemisphere of flux having an inward (positive x) component of direction, and similarly J is composed of the hemisphere of flux having an outward (negative x) component of direction. This reduces the problem to one dimension.

On passing through an infinitesimal layer dx, a fraction KIdx of the flux I will be absorbed and a fraction SIdx will be lost by scattering in a backward direction. On the other hand, a quantity SJdx will be added by scattering from the flux J. Sideward scattering is disregarded with the assumption that any sideward loss of radiant energy is compensated by an equal contribution from the neighboring parts of the layer. In addition, by Kirchhoff's law, this layer, dx, will contribute by radiating the amount KEdx, where E designates the blackbody radiation at the temperature and wavelength in question.

By adding these quantities we obtain –

$$\frac{dI}{dx} = -(K + S)\, I + SJ + KE \qquad 1)$$

$$\frac{dJ}{dx} = (K + S)\, J - SI - KE \qquad 2)$$

With the assumption that the temperature in the slab is uniform, the equations have been integrated to obtain the general solution:

$$I = A(1 - \beta)\, e^{\sigma x} + B(1+ \beta)\, e^{-\sigma x} + E \qquad 3)$$

$$J = A(1 + \beta)\, e^{\sigma x} + B(1- \beta)\, e^{-\sigma x} + E \qquad 4)$$

where A and B are constants dependent on the boundary conditions and

$$\sigma = \left[K(K+ 2S)\right]^{1/2} \qquad 5)$$

$$\beta = \left[K/(K + 2S)\right]^{1/2} \qquad 6)$$

Both σ and β are taken to be the positive roots.

If the continuous medium has a refractive index different from 1, then surface or specular reflectance has to be considered. For the present we confine the treatment to a body of particles suspended in air, so that only a diffuse boundary is present and surface reflectance can be neglected. With this restriction, equations for the boundary conditions have been derived from the general solution as follows:

With no radiation incident on either side, the emittance ϵ for a slab of thickness D is –

$$\epsilon = \frac{Jo}{E} = \frac{I_D}{E} = \frac{2\beta\left[(1+\beta)\, e^{\sigma D} + (1-\beta)e^{-\sigma D} - 2\right]}{(1+\beta)^2 e^{\sigma D} - (1-\beta)^2 e^{-\sigma D}} \qquad 7)$$

If the slab is thick enough to be opaque, this reduces to –

$$\epsilon = \frac{Jo}{E} = \frac{I_D}{E} = \frac{2\beta}{1+\beta} \qquad 8)$$

Also, it can be shown that

$$K/S = \frac{(1-R_\infty)^2}{2R_\infty} \qquad 9)$$

where R_∞ is the diffuse reflectance of the opaque slab.

With diffuse incident radiation Io, the radiation from the slab on the transmission side is –

$$I_D = \frac{Io(4\beta) + E(2\beta)\left[(1+\beta)e^{\sigma D} + (1-\beta)e^{-\sigma D} - 2\right]}{(1+\beta)^2 e^{\sigma D} - (1-\beta)^2 e^{-\sigma D}} \qquad 10)$$

On the reflection side the radiation, including that emitted, is —

$$Jo = \frac{Io\,(1-\beta^2)\,(e^{\sigma D} - e^{-\sigma D}) + E(2\beta)\,[(1+\beta)e^{\sigma D} + (1-\beta)e^{-\sigma D} - 2\,]}{(1+\beta)^2 e^{\sigma D} - (1-\beta)^2 e^{-\sigma D}} \qquad 11)$$

The last two equations apply to a translucent emitter in a burner in which the emitter receives radiation Io from some other emitter.

If the slab has an underlayer of reflectivity r at x = D, then —

$$Jo = \frac{Io[1-\beta^2 - r(1-\beta)^2][e^{\sigma D} - e^{-\sigma D}] + E(2\beta)\{[1+\beta-r(1-\beta)]\,e^{\sigma D} + [1-\beta-r(1+\beta)]e^{-\sigma D}\}}{(1+\beta)^2 - r(1-\beta^2)\;e^{\sigma D} - (1-\beta)^2 - r(1-\beta^2)\;e^{-\sigma D}} \qquad 12)$$

When Io = 0 this reduces to —

$$\epsilon = \frac{Jo}{E} = \frac{(2\beta)\{[1+\beta-r\,(1-\beta)]\,e^{\sigma D} + [1-\beta-r\,(1+\beta)]\,e^{-\sigma D}\}}{[(1+\beta)^2 - r(1-\beta^2)]e^{\sigma D} - [(1-\beta)^2 - r(1-\beta^2)]\,e^{-\sigma D}} \qquad 13)$$

This case occurs in some of our emittance and reflectance determinations.

For a consolidated material the dielectric is the continuous phase and specular reflection must be taken into account. In the differential equations we must replace E by n^2E, but to avoid confusion, we will indicate the (internal) absorption coefficient by K' rather than K. The relation between the two coefficients will be discussed later. Let ρ_i be the internal diffuse (hemispherical illumination-hemispherical collection) reflectance and ρ_e the external diffuse reflectance at the surface of the slab. According to Klein, the expressions for diffuse reflectance R (including both surface and internal reflection), transmittance T, and emittance ϵ, with hyperbolic functions substituted for exponentials, are (10) —

$$R = \frac{[(1-\rho_i)^2 - \beta^2(1-\rho_i-2\rho_e)(1+\rho_i)]\,\sinh \sigma D + 2\beta\,(\rho_e+\rho_i)(1-\rho_i)\,\cosh \sigma D}{[\beta^2(1+\rho_i)^2 + (1-\rho_i)^2\,]\sinh \sigma D + 2\beta(1-\rho_i^2)\;\cosh \sigma D} \qquad 14)$$

$$T = \frac{2\beta(1-\rho_e)(1-\rho_i)}{[\beta^2(1+\rho_i)^2 + (1-\rho_i)^2\,]\,\sinh \sigma D + 2\beta(1-\rho_i^2)\;\cosh \sigma D} \qquad 15)$$

$$\epsilon = \frac{2\beta(1-\rho_e)[\beta(1+\rho_i)\;\sinh \sigma D + (1-\rho_i)\;(\cosh \sigma D - 1)\,]}{[\beta^2\,(1+\rho_i)^2 + (1-\rho_i)^2\,]\,\sinh \sigma D + 2\beta\,(1-\rho_i^2)\,\cosh \sigma D} \qquad 16)$$

If the slab is thick enough to be opaque, the expression for emittance reduces to —

$$\epsilon = \frac{2\beta(1-\rho_e)}{1+\beta-\rho_i\,(1-\beta)} = \frac{2n^2\beta(1-\rho_i)}{1+\beta-\rho_i\,(1-\beta)} \qquad 17)$$

The latter form is a consequence of the equilibrium relationship

$$1 - \rho_e = n^2(1-\rho_i) \qquad 18)$$

The hemispherical external reflectance for a plane surface with diffuse illumination can be calculated from the refractive index. This is most easily done by means of Walsh's equation, which he obtained by integration of the Fresnel equations for oblique incidence (11, 12). Corresponding values of ρ_i can then be obtained by Equation 18. It does not appear that ρ_i or ρ_e for a plane surface is greatly different from that for a surface with shallow roughness, especially in the visible and near infrared region where dielectrics are only weakly absorbing (13). Furthermore, it turns out that the expression for emittance of opaque dielectric bodies is quite insensitive to the value of ρ_i, as shown by Richmond and also confirmed experimentally (11).

The foregoing expressions have all been derived for total hemispherical flux. Measurements, however, are usually directional, at least in part. Thus, reflectance measurements discussed later in this report are either with directional illumination and hemispherical illumination and directional viewing. Directional emittance is the complement of these. The data from such measurements are customarily treated with the Kubelka-Munk theory as if they were hemispherical rather than directional. Our data also have been treated in this way.

Relations Between K-M and Intrinsic Absorption Coefficients

Now let us consider the relationship between the different absorption coefficients: K for dispersed material, K' for consolidated material, and α the intrinsic coefficient, which is the one measured on clear material with corrections to exclude the effect of surface reflectance. To obtain a common basis we express all coefficients in units of sq cm/g instead of cm^{-1}; x then is the g/sq cm. Consider a single particle in the case of the dispersed material. (A fiber disposed crosswise to the flux can be treated similarly.) Here we limit ourselves to particles and wavelengths such that absorbency is low and the differential form of expression is accurate enough that bulk optical properties still apply. From Mie scattering calculations it appears that for thoria, with a refractive index of about 2, the limit for this is a diameter of one-third the wavelength (14). We envisage a hemispherical beam, I, incident on the particle. A fraction ρ_e of the beam I is reflected from the particle. The remainder traverses the particle with an average path length l_1, then is partly transmitted and partly internally reflected. The fluxes and absorptions of this and succeeding traverses are as follows:

	In Transit	Absorbed	Reflected
1st Traverse	$I(1-\rho_e)$	$I(1-\rho_e)\ l_1 d\alpha$	$I(1-\rho_e)\rho_i$
2nd Traverse	$I(1-\rho_e)\ \rho_i$	$I(1-\rho_e)\ \rho_i l_2 d\alpha$	$I(1-\rho_e)\rho_i^2$
3rd Traverse	$I(1-\rho_e)\ \rho_i^2$	$I(1-\rho_e)\ \rho^2_i l_3 d\alpha$	$I(1-\rho_e)\ \rho_i^3$

and so on, where d is density, so that ld has the dimensions of x. If $l_1 = l_2 = l_3 = l_n$, then the total absorption by the particles is —

$$\frac{I(1-\rho_e)\, l\, d\alpha}{1-\rho_i} = In^2 l d\alpha \qquad 19)$$

A similar expression in which I is replaced by E is obtained when we consider emission.

We wish to sum the absorption over all particles encountered by the hemispherical beam, I, in traversing the differential, dx. In addition to the assumption made above as to the equality of path lengths of the reflections inside the particle, we also assume that refraction at the surface of the particles does not affect the ratio of average path length to the amount of material. One method of visualizing this question is to consider the division of bulk material into space-filling cells such as cubes and octahedrons followed by separation of the cells. We are assuming that the average path length after separation is the same as before separation. This is perhaps not true when the particles have forms such as spheres or cylinders (except at their midsections). We think it is more likely to be true when the particle surface is highly irregular. Later in this paper we show that mantle fibers are very irregular in cross section.

In addition, note that the number of particles encountered by a directional beam varies with the angle that it makes with the x-direction. Note also that we must average the path according to the intensity of the beam components in the different directions. We obtain an average path length, $d\Sigma l = Ldx$, where L is the dimensionless ratio of average path length to dx. This gives us $IKdx = In^2 L\alpha dx$ or $K = n^2 L\alpha$. Kubelka has shown that, if the radiation is perfectly diffuse (has the same intensity in all directions), then L =2 (15).

In the case of consolidated material the similar relationship is $K' = L\alpha$. In this case too, the components of the beam traveling at an angle to x have a longer path than those traveling along x, and again L = 2 for perfectly diffuse radiation.

Another effect needs consideration. As pointed out by Klein, the path of part of the radiation entering and leaving the element, dx, in a given direction may actually be a circuitous one, longer than would be expected according to the geometry (10). No data on the magnitude of this effect have come to our notice in the literature. If we ignore this effect and take L = 2, we have —

$$K' \text{ (absorption coefficient for consolidated material)} = 2\alpha \qquad 20)$$

$$K \text{ (absorption coefficient for dispersed material)} = 2n^2\alpha \qquad 21)$$

$$K = n^2 K'$$

Refractive Index

The refractive index thus enters calculations of emittance. Furthermore, the refractive index is the physical constant, which, along with microstructure, controls scattering. Thus the variation of the refractive index with temperature is a matter of some importance. Ramaseshan et al. have reviewed the relevant theory and data in the visible region (16). It appears that variation of the refractive index of metal oxides in the visible is quite small, amounting to no more than 0.02/1000°C for magnesium oxide. Less data available on its variation in the infrared. Results of one study (again on magnesium oxide) show very little variation at 12.5μm when the temperature increases from 8.5° to 950°K; however, when the temperature increases to 1950°K, the refractive index increases from about 0.87 to about 0.94 (17). Thus it seems likely that the temperature dispersion of the refractive index of thoria and other oxides should increase with wavelength but not to more than about 10%/1000°C at 12μm.

The small variation of the refractive index with temperature indicates that scattering coefficients ordinarily should not vary appreciably with temperature. However, the broadening of the ceria absorption band in the visible with temperature rise will be accompanied by an increase in the refractive index in the neighboring higher wavelength range.

Procedures for Measurement of Radiation Properties

Materials

Mantles used in this study were of single-stitch weave, obtained from the Welsbach Corporation. Mantles of normal ceria content were from commercial production; those with no ceria and nominally 3 times the normal amount of ceria were supplied on special request. Chemical analyses of the mantle fabrics (excluding the neck portion) are shown in Table 1.

Table 1. CHEMICAL ANALYSIS OF MANTLE FABRIC SAMPLES

	Zero Ceria	Normal Ceria	Thrice Normal Ceria
	wt %		
Al_2O_3	0.25	0.32	0.25
BeO	0.09	0.09	0.11
CeO_2	0.00	0.61	3.26
MgO	0.05	0.11	0.11
SiO_2	0.60	0.29	0.61

Determination of Kubelka-Munk (K-M) Coefficient at Room Temperature

These measurements were made at the IIT Research Institute (IITRI). A General Electric Co. spectrophotometer equipped with a diffuse reflectance attachment was used for wavelengths from 0.38 to 0.7μm. Measurements were extended to 2.4μm with a laboratory-constructed instrument consisting of an integrating sphere attached to a Perkin-Elmer single-beam monochromator with a lead sulfide detector.

To prepare the fabric the collodion coating of the hard mantles was burned off, the top of the mantle cut off, and the remaining fabric cut lengthwise into two equal parts. We flattened the fabric by placing it on a flat stainless steel screen and by impinging the air-natural gas flame of a hand torch on it. The pieces of fabric were then cut to size and weighed.

To determine the Kubelka-Munk coefficients, one reflectance spectrum (R_∞) is obtained with a sample thick enough to be opaque, and another, R_o, is obtained with a thinner sample backed by a black cavity. The latter sample must be thin enough to show a substantial difference from R_∞. On the other hand, several layers of mantle fabric had to be used to reduce the area of holes and increase the uniformity of effective thickness. Five layers of the single-stitch mantle fabric gave satisfactory results. Change in orientation of the layers to one another did not affect the results. Use of four layers gave reasonably close agreement, which indicated that five layers were enough to obtain uniformity of thickness.

The values of SX were obtained from the two reflectance values by means of a Kubelka-Munk chart (18). Values of K/S were obtained from a chart or table of K/S against R_∞ that had been calculated by means of Equation 9.

Emittance Determinations

Normal emittance measurements were made at IITRI with an apparatus in which the sample and a silicon carbide plate (used as a standard) are mounted side by side in a tube furnace and continuously moved back and forth along the length of the furnace (19) (Figure 2). For readings, a cooled shield is inserted at the center of the furnace as close to the traversing sample as possible. The radiation emitted is dispersed and measured by a Perkin-Elmer spectrophotometer with sodium chloride optics. Mantle fabric for these determinations was prepared by the method described above. The pads of fabric were mounted on the vertical-facing alumina tray of the apparatus by clamps of rhodium sheet placed along the sides and bottom of the sample and cemented to the tray.

Cooling of the sample as it comes before the cooled shield was investigated as a source of error. It was feared that the mantle fabric would cool much faster than the standard because of its unconsolidated nature and resulting inaccessibility of heat stored in adjacent layers.

Rate-of-cooling data were obtained by stopping the sample or standard in front of the port for about 10 seconds while the emission was being recorded. The rate of signal decrease in percent of the initial signal per second is shown in Figure 3 plotted against wavelength.

At each wavelength the emitted radiation to which the signal is directly proportional is considered to be the product of the emittance and the radiative power of a blackbody. The emittance remains substantially constant as the sample or standard cools during the 10-second period since only a small temperature change occurs. The rate of signal decrease can then be expressed as —

$$\frac{1}{S_\lambda}\frac{dS_\lambda}{dt} = \frac{1}{E_\lambda}\frac{dE_\lambda}{dT}\frac{dT}{dt} \qquad 23)$$

where dS_λ/dt is the experimental rate of decrease, E_λ is the radiative power of a blackbody at wavelength λ, T is temperature, and t is time. Values of $\frac{dE_\lambda}{E_\lambda dT}$ have been calculated from the Planck equation and plotted in Figure 3 with dT/dt evaluated to make the curve pass through the experimental point for the silicon carbide at 2μm. The experimental points for the silicon carbide standard follow the theoretical curve satisfactorily. The mantle fabric, on the other hand, shows a greater rate of signal decrease at the longer wavelengths and a slower rate at the short wavelengths. However, at wavelengths above 1μm indicated rates of cooling of sample and standard are of about the same magnitude. The actual cooling period was less than 2.5 seconds, which was the time of traversal of the 1-1/4-in. sample width. Error from this period of cooling did not appear to be serious, except at wavelengths below 2μm.

The effect of sample-to-port distance was also investigated. As this distance increases, more radiation from the furnace wall can strike the front surface of the sample and be reflected into the measurement beam. The amount of radiation reflected from the sample is greater than that from the standard because the mantle fabric has greater reflectance than the standard. Also, more of the radiation, which strikes sample and standard at a high angle of incidence, is reflected specularly by the standard than by the sample; the specular component is not included in the beam collected by the monochromator. Measurements were made at several different wavelenths with sample-to-port distance varied from 1/16 to 1/4 in. Emittance values increased at the rate of 0.05 per 1/16 in. and 2 to 4 m, and a slightly higher rate at higher wavelengths. Because of unevenness of the sample surface and variation in the sample mounting and tracking, it was not possible to reduce the estimated sample-to-port distance below about 1/16 in. Thus there is an uncertainty of about 0.05 in emittance values. We think the observed values are likely to be too high rather than too low, except at wavelengths from 1 to 2 μm where error from cooling may have more effect.

Emittance measurements were made on 12-layer samples of mantle fabric backed by the alumina sample tray, and on 4-layer samples backed by silicon carbide of known emittance.

In treatment of the data, the 12-layer samples were assumed to be thick enough to be opaque; this may not be strictly true, but the situation is helped by the fact that the emittance of the alumina tray is low (similar to that of thoria) in the low-wavelength region where the mantle fabric is most translucent. Absorption and scattering coefficients were calculated by application of Equations 8 and 12.

Reflectance Measurements

Some reflectance measurements were also obtained at the National Bureau of Standards. Two instruments were used. In one a laser is used as a source of radiation (20). Illumination is at 12 degrees from the normal; an integrating sphere is used to collect the reflected radiation. Measurements could be made at temperatures from ambient to about 1900°C in vacuum, or to about 1400°C in air, but only at wavelengths of 0.6328 and 1.15μm. In this instrument, at least for measurements at elevated temperature, the sample is required to be in the form of a consolidated disk of 1/2-in. diameter.

We prepared samples for measurement on this instrument by grinding the mantle fabric for about 15 minutes on a motorized mortar and pestle; pressing the powder, lubricated with a few drops of a 2.5% aqueous solution of polyvinyl alcohol, in a die at about 12,000 psi; and sintering. The time of sintering was 2 hours, and the atmosphere was air. The temperature of sintering was adjusted to obtain about the same density on each sample: 1270°-1290°C for the sample with no ceria, 1230°-1260°C for the sample with normal ceria, and 1180°-1200°C for the sample with thrice-normal ceria. Densities obtained were 5.10, 5.05, and 5.29 g/cu cm.

The other instrument used at NBS was a Cary-White Model-90 recording spectrophotometer with a diffuse reflectance attachment that operates over the spectral range 2.5 to 22.2μm and at temperatures from 20° to 1000°C (21). The specimen in the form of powder is irradiated hemispherically and viewed at a direction of 20° from the normal to the sample surface. Temperature of the sample is monitored by a thermocouple probe. Powder for these determinations was prepared by grinding the fabric for 15 minutes under water in a motorized mortar and pestle.

Results of Experimental Measurements

Refractive Index

A specimen of fused thoria made by the Norton Company was obtained from W. E. Danforth of the Bartol Research Foundation; a prism was cut from it and polished at the IIT Research Institute. The refractive index was determined at Eastman Kodak Company at room temperature by the minimum deviation method. Kodak estimated the accuracy to be $\pm 5 \times 10^{-3}$. The results are shown in Table 2.

Table 2. REFRACTIVE INDEX OF THORIA

Wavelength, μm	Refractive Index	Wavelength, μm	Refractive Index
0.405	2.1485	3	2.0415
0.436	2.1354	4	2.0214
0.486	2.1200	5	1.9952
0.546	2.1076	6	1.9657
0.593	2.1010	7	1.9254
0.656	2.0930	8	1.8744
1	2.0698	9	1.8148
2	2.0554		

Microstructure of Mantle Materials

The microstructure of filaments of a single-stitch mantle mounted in an epoxy resin is shown in the photomicrograph in Figure 4. This is a cross section of filaments of two adjacent threads crossing at a small angle. The streaks in the photomicrograph are diffuse light reflected from filaments buried in the resin. The diameter of the filaments is about 10μm; the extreme irregularity and hollows of the cross section probably greatly increase the scattering at wavelengths below about 6μm.

The weight of the mantle fabric was 0.011 g/sq cm. Holes in the fabric amount to about one-half of the area, so that the actual thickness of the threads of a single layer of mantle fabric varies from about 0.02 to about 0.04 g/sq cm where the threads cross.

A photograph of an experimental Thermacomb mantle (from the 3M Company) is shown in Figure 5. The material is an open three-dimensional network composed of straight members 1 to 3 mm long joined to form irregular polygons. In the form shown it serves as a mantle; in flat sheets it could serve as the radiator of a porous plate burner.

The connecting members of this material are triangular and hollow in cross section, with an effective thickness several times the thickness of a thread of an ordinary mantle. This is a probable explanation for the lower ceria content (about 0.2%) reported to be optimum for light emission in this mantle (22), compared with about 1% in ordinary mantles.

Absorption and Scattering Coefficients

Absorption and scattering coefficients obtained from the reflectance measurements at room temperature over the wavelength range 0.4 to 2.4μm are shown in Figure 6 and 7. Each point represents the average results for two or three samples.

The general trend of absorption coefficients is as expected; however, there is no consistent trend with ceria content except at wavelengths below 0.42μm, where the effect of the ceria absorption band predominates. Both absorption and scattering coefficients are less accurate at the higher wavelengths where the reflectance is above 90% and where there is less difference between the two reflectance readings. The scattering coefficients for the different ceria contents are very nearly the same, and the differences do not appear to be significant. The increase in scattering coefficients with wavelength in the range from 0.8 to 2.4μm is unexpected.

Emittance values obtained on the mantle fabric with three different levels of ceria content are shown in Table 3. Results agree well, with no significant difference among the three samples at wavelengths from 1 to 6μm. We attribute differences at higher wavelengths to experimental error.

Table 3. INFRARED EMITTANCE OF MANTLE FABRIC AT 1200°C

	Thoria Having				
	No Ce	3X Normal Ce	Normal Ce		
Wavelength, μm	12 Layer	12 Layer	12 Layer	4 Layer	SiC*
	Emittance				
1	0.09	0.09	0.10	0.26	0.74
1.5	0.11	--	0.115	0.31	0.85
2	0.12	0.14	0.14	0.34	0.92
3	0.13	0.15	0.14	0.32	0.90
4	0.14	0.15	0.15	0.32	0.88
4.5	--	--	0.17	0.32	0.875
5	0.17	0.17	0.19	0.32	0.87
6	0.20	0.21	0.225	0.335	0.87
7	0.22	0.24	0.28	0.36	0.865
8	0.28	0.32	0.355	0.45	0.87
9	0.41	0.44	0.51	0.615	0.84

* Reference values, determined against a blackbody.

An emittance spectrum (Table 3) from four layers of mantle fabric backed by a silicon carbide plate was obtained from a sample of fabric having normal ceria content. Absorption and scattering coefficients at wavelengths from 2 to 8μm were calculated from the spectra of the two (12-layer and 4-layer) samples.

Scattering coefficients ranged from 40 to 55 sq cm/g (average 50) and had no significant trend with wavelength. As noted previously, we do not expect the scattering coefficient to vary with temperature. When the possibilities of error in the emittance determinations are considered, this value is in remarkable agreement with the coefficients determined at room temperature.

The absorption coefficient spectrum from these emittance determinations is shown in Figure 8, together with the visible-near infrared spectrum obtained on the same kind of mantle fabric at room temperature. In the near infrared where the curves overlap, the high-temperature absorption coefficient is greater than the low-temperature coefficient by a factor of about 2, which we consider a reasonable value. However, it should be noted that the calculated absorption coefficient has a high rate of change with change in emittance. With the scattering coefficient assumed to be constant, an increase from 0.14 to 0.19 in emittance is equivalent to a doubling of the absorption coefficient by a factor of 2.6. These factors correspond to the estimated maximum error of the emittance determination.

A comparison of our K's with those calculated from Weinrich's intrinsic absorption coefficients provides us with a test of our theoretical relationship. Values were obtained at 0.4 and 0.66μm according to the formula $K = \frac{2n^2}{d}\alpha$ as follows:

Wavelength, μm	Intrinsic Absorption Coefficient, cm^{-1}	Refractive Index	K-M Absorption Coefficient, sq cm/g	
			Calculated	Observed
0.4	8	2.15	7.4	4.8
0.66	3	2.09	2.6	1.3

The density of thoria was taken as 10.0 g/cu cm. Values of the intrinsic absorption coefficient were those for the red material, heated at 1000°C in air. Values for material heated at 1000°C in vacuum are lower and would give closer agreement. We are uncertain as to the exact oxidation state of the mantle fabric, which had been heated in an oxidizing flame. The agreement shown appears reasonable in consideration of the assumptions made in the theory and of the experimental accuracy.

Reflectance Measurements at National Bureau of Standards

Results of reflectance determinations made at NBS in the infrared on powder samples are shown in Figure 9 in the form of emittance spectra. The emittance here is a directional one, at a 20 degree angle from the normal. This is calculated, according to Kirchhoff's law, as the complement (1–R) of the reflectance determined with hemispherical illumination and 20 degree viewing. Reflectance was determined both at 20° and 1000°C on mantle material with normal ceria content, and at 1000°C on mantle material with zero ceria and with thrice-normal ceria. We attribute the anomalous peaks in the 20°C spectrum in the wavelength range 2.5 to 8μm to adsorbed water and other adsorbed impurities. These should not be present in the 1000°C spectra. The origin of the small peaks still present in the 1000°C spectra is not known. The emittance from 2.5 to 5μm is much lower than values obtained at 1200°C on consolidated material (8), which indicates the effect of scattering by the powder.

Reflectance spectra were also obtained at NBS on powder samples of different thicknesses, backed by a black diffusing paint surface, in an attempt to determine absorption and scattering coefficients. The temperature was raised to 250°C to decrease the amount and effect of adsorbed material. A higher temperature would have endangered the paint backing. However, effects of adsorption were still quite appreciable, and results were not consistent enough to obtain coefficients. It appears that measurements at elevated temperature on mantle fabric (rather than on powder) would give us a better chance of obtaining the coefficients. The lesser scattering power of the fabric would give lower reflectance and a slower rate of change of K/S with reflectance.

Reflectance values, R, from the NBS laser instrument and values of K's/S calculated by means of Equation 17 are shown in Table 4. [Values of ρ_e were obtained from the Walsh equation with room-temperature values of the refractive index (11).] Measurements were made at 20°C, near 1000°C, and near 1200°C. A second measurement at 20°C, after the high-temperature measurements, indicates the effect of changes in the material such as further sintering or change in oxygen content. Standard deviations of the reflectance measurements ranged from 0.001 to 0.004.

These measurements do not show the substantial drop in K'/S in going from 0.6328 to 1.15μm that was found in K/S in the IITRI measurements on mantle fabric (Figure 6). This may be caused by a large change in the scattering coefficient of the consolidated and sintered material with change in wavelength. No data are available on this point. However, variation of K'/S with temperature should not be affected. This allows us to calculate absorption coefficients for mantle fabric at elevated temperature at these two wavelengths. We assume that the scattering coefficient of the sintered sample is constant with temperature and thus that the change in absorption coefficient with temperature, determined on the sintered material, also applies to mantle fabric. Absorption coefficients at 1200°C and at 0.6328 and 1.15μm have been calculated for mantle fabric of normal ceria content using these assumptions. The values, as shown in Figure 8, line up well with the infrared values at 1200°C obtained from emittance determinations.

Table 4. RADIATION PROPERTIES OF SINTERED MANTLE MATERIAL

No Ceria				Normal Ceria				Thrice Normal Ceria			
Temp, °C	R	K'/S	Relative K'/S	Temp, °C	R	K'/S	Relative K'/S	Temp, °C	R	K'/S	Relative K'/S
At 0.6328 μm											
20	0.712	0.0046	1.00	20	0.768	0.0025	1.00	20	0.738	0.0035	1.00
990	0.697	0.0053	1.14	985	0.724	0.0041	1.61	965	0.637	0.0094	2.69
1230	0.668	0.0071	1.54	1220	0.661	0.0076	3.00	1190	0.511	0.0292	8.32
20*	0.728	0.0039	--	20	0.781	0.0022	--	20	0.742	0.0034	--
At 1.15 μm											
20	0.691	0.0059	1.00	20	0.744	0.0034	1.00	20	0.741	0.0036	1.00
1110	0.663	0.0077	1.30	985	0.694	0.0058	1.68	1015	0.669	0.0073	2.05
1235	0.629	0.0106	1.79	1220	0.664	0.0076	2.22	1210	0.610	0.0126	3.54
20	0.689	0.0061	--	20	0.756	0.0030	--	20	0.736	0.0037	--

* Measurement repeated after high-temperature measurements.

The temperature coefficients increase with increasing ceria content at both 0.6328μm and 1.15μm. The great increase with ceria content at 0.6328μm can be attributed to the effect of the ceria absorption band.

Discussion

A graph of the emittance function (Equation 7) for dispersed material is shown in Figure 10 for a wide range of thickness and for several decades of the scattering and absorption coefficients. Several observations are worth noting. First, it is apparent that the effect of absorptivity can, under some conditions, be interchanged with the effect of thickness. Thus, when the section is thin enough (how thin depends on both coefficients), the emittance is simply the product of the thickness and the absorption coefficient. The ceria content of mantle material has a large effect on its absorption coefficient in the visible part of the spectrum. It should not be surprising, then, that the optimum ceria content should depend on the effective thickness of the mantle.

The scattering coefficient also can have important effects. For example, we can show that for optically opaque specimens, those so thick that additional thickness does not change the emittance, the emittance depends solely on the ratio of the absorption coefficient to the scattering coefficient. Although the absorption coefficient depends mainly on the chemical composition and crystal structure of the material at the atomic level, the scattering coefficient depends on the microstructure, particularly on the presence and number of boundaries in the material where a change in the refractive index occurs. For particles dispersed in an otherwise homogeneous medium, the scattering coefficient depends mainly on the size, shape, and refractive index of the particles relative to the medium. For consolidated ceramic materials, it depends mainly on the number, size, shape, and relative index of the particles of different phases, including pores, in the material. In anisotropic crystalline materials, crystallite boundaries also contribute to scattering. In some cases, variation of the microstructure within the mechanical requirements provides another means of obtaining desired properties of radiators.

Now let us consider the position of the mantle in this picture. The weight of a single layer of the single-stitch mantles used in our investigation was 0.011 g/sq cm. We see the emission from two layers of fabric when we look at the center portion of an ordinary cylindrical upright mantle. The actual thickness in the path of a ray may vary from zero to perhaps 0.08 g/sq cm for a ray through crossed threads in both layers. From Figure 10, we see that at this thickness the emittance is equal, with little deviation, to the product of the absorption coefficient and average thickness, for absorption coefficients up to about 2 sq cm/g. Emittance of two layers of mantle fabric at several different wavelengths in the infrared have been calculated from the absorption coefficients of Figure 8 and are shown in Figure 10. These emittance values are compared below with those from Ives and coworkers (2) and from Rubens (23). With consideration of the possible differences in mantle composition and weight, good agreement is shown at wavelengths below 8μm.

Wavelength, μm	This Work	Ives et al. (2)	Rubens (23)
	Emittance		
2	0.011	0.01-0.02	0.007
3	0.011	0.01-0.02	0.0088
5	0.026	0.03	0.014
8	0.11	0.3	0.211

We do not know how to account for the apparently low emittance values we found at wavelengths of 8μm and above. Alternatively, at wavelengths from about 0.6 to about 6μm the absorption coefficient can apparently be calculated from an emittance spectrum, such as that of Rubens or Ives et al., by use of an average fabric weight. At shorter wavelengths the absorption coefficient can still be estimated by application of the known scattering coefficient (Equation 7) and an estimated effective thickness. At longer wavelengths the same method could be used, but the scattering coefficient is not known here.

ACKNOWLEDGMENTS

This work was sponsored by the American Gas Association. The author is grateful to it for permission to publish this paper.

Also we wish to thank Mr. O. H. Olson of IIT Research Institute for advice and for supervision of measurements made there; similarly, we wish to thank Mr. J. C. Richmond and Dr. V. Wiedner of the National Bureau of Standards for their contributions.

Literature Cited

1. Rubens, H., "Emittance and Temperature of Welsbach Mantles With Different Ceria Contents," Ann. Phys. 18, 725 (1905).

2. Ives, H. E., Kingsbury, E. J., and Karrer, K., "A Physical Study of the Welsbach Mantle," J. Franklin Inst. 186, 401-38, 585-625 (1918).

3. Rutgers, G.A.W., "Temperature Radiation of Solids," in Flugge, S., Ed., Handbuch Der Phys. Vol. 24, 168. Berlin: Springer, 1958.

4. Ritzow, G., "The Heat Radiation of Glowing Oxides and Oxide Mixtures in the Infrared Region," Ann. Phys. 19, 769-99 (1930).

5. Liebman, G., "The Temperature Radiation of Colorless Oxides in the Visible," Z. Physik 63, 404-36 (1930).

6. Weinrich, O. A., and Danforth, W. E., "Optical Properties of Crystalline Thoria," Phys. Rev. 88, 953-54 (1952).

7. Gryvnak, D. A. and Burch, D. E., "Optical and Infrared Properties of Al_2O_3 at Elevated Temperatures," J. Opt. Soc. Amer. 55, 625 (1965).

8. Clark, H. E. and Moore, D. G., "A Rotating Cylinder Method for Measuring Normal Spectral Emittance of Ceramic Oxide Specimens From 1200° to 1600°K," J. Res. NBS 70A, 393-415 (1966).

9. Hamaker, H. C., "Radiation and Heat Conduction in Light-Scattering Material," Philips Res. Rep. 2, 55-67 (1947).

10. Klein, J. D., "Radiation Heat Transfer Through Scattering and Absorbing Nonisothermal Layers," in Katzoff, S., Ed., Symposium on Thermal Radiation of Solids, NASA SP-55, 73-81. Washington, D.C.: Govt. Print. Office, 1965.

11. Richmond, J. C., "Effect of Surface Roughness on Emittance of Nonmetals," J. Opt. Soc. Amer. 56, 253-54 (1966).

12. Richmond, J. C., "Relation of Emittance to Other Optical Properties," J. Res. NBS 67C, 217-26 (1963).

13. Giovanelli, R. G., "A Note on the Coefficient of Reflection for Internally Diffuse Light," Opt. Acta 3, 127-30 (1956).

14. Plass, G. N., "Mie Scattering and Absorption Cross Sections for Aluminum Oxide and Magnesium Oxide," Appl. Opt. 3, 867-72 (1964).

15. Kubelka, P., "New Contributions to the Optics of Intensely Light-Scattering Materials. Part 1," J. Opt. Soc. Amer. 38, 448-57 (1948).

16. Ramaseshan, S., Vedam, K. and Krishnan, R. S., "Thermo-Optic Behavior," in Krishnan, R. S., Ed., Progress in Crystal Physics, Vol. 1, 139-67. Madras, India: S. Viswanathan, 1958.

17. Jasperse, J. R. et al., "Temperature Dependence of Infrared Dispersion in Ionic Crystals LiF and MgO," Phys. Rev. 146, 526-42 (1966).

18. American Society for Testing and Materials, "Standard Method of Test for Reflectivity and Coefficient of Scatter of White Porcelain Enamels," ASTM Designation: C347-57, in 1966 Book of ASTM Standards, Part 13, 312-15. Philadelphia, 1966.

19. Olson, O. H. and Katz, S., "Emissivity, Absorptivity, and High-Temperature Measurements at Armour Research Foundation," in Claus, F. J., Ed., Surface Effects of Spacecraft Materials, 164-81. New York: John Wiley, 1960.

20. Kneissl, G. J. and Richmond, J. C., "A Laser-Source Integrating Sphere Reflectometer," U.S. NBS Tech. Note 439 (1968) February.

21. White, J. V., "New Method of Measuring Diffuse Reflectance in the Infrared," J. Opt. Soc. Amer. 54, 1332-37 (1964).

22. Stack, T. N. and Manske, W. J., "Development of the Thermacomb Gas Light Mantle." Paper presented at the American Gas Association Research and Utilization Conference, Cleveland, June 2-4, 1964. Cat No. M31460.

23. Rubens, H., "Concerning the Emittance Spectrum of Welsbach Burners," Ann. Phys. 18, 725-38 (1905).

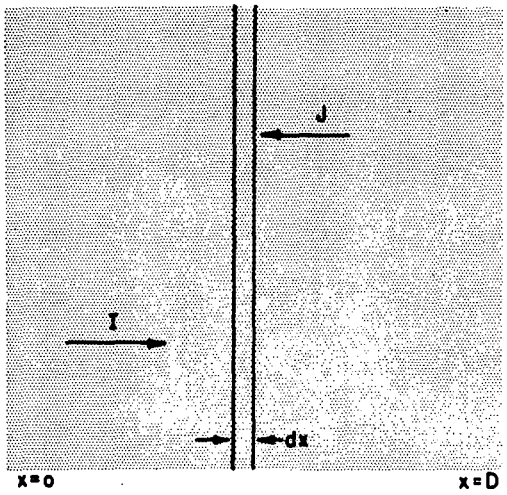

Figure 1. RADIANT FLUX OF UNIFORM ONE-DIMENSIONAL SLAB

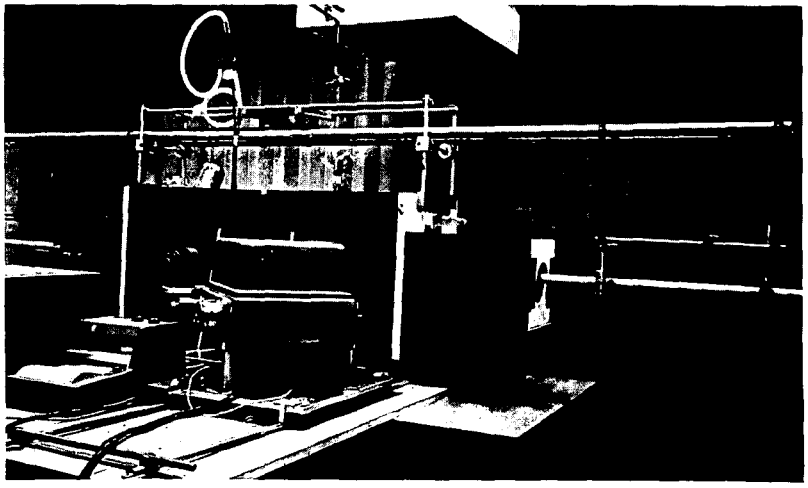

Figure 3. EMITTANCE MEASUREMENT APPARATUS

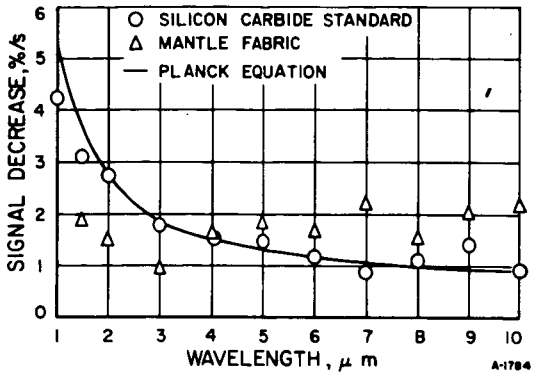

Figure 3. EFFECT OF SAMPLE COOLING

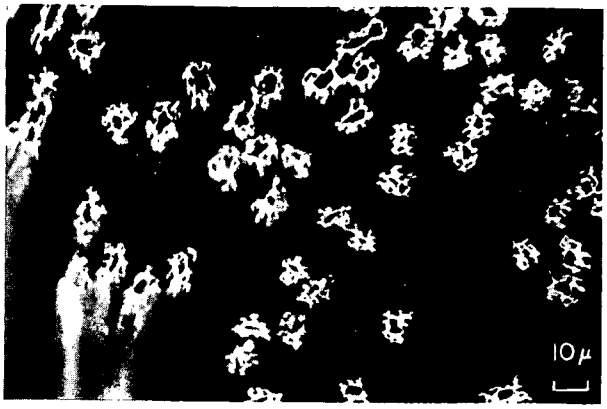

Figure 4. PHOTOMICROGRAPH OF CROSS SECTION OF SINGLE-STITCH MANTLE FABRIC

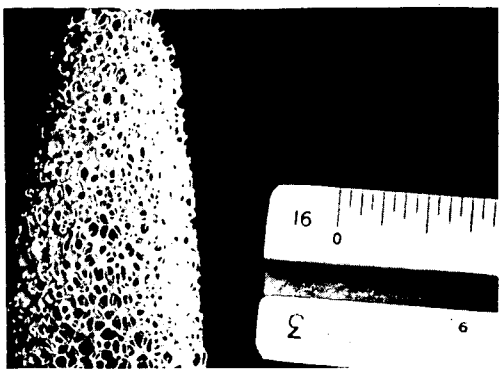

Figure 5. EXPERIMENTAL THERMACOMB MANTLE

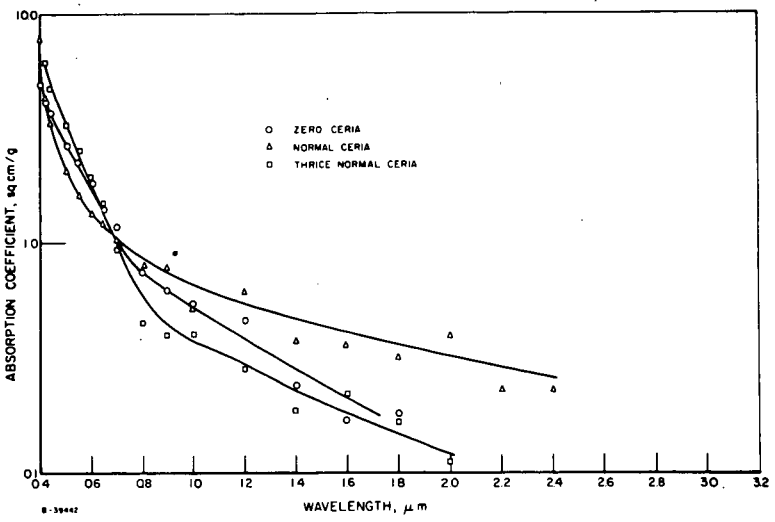

Figure 6. ABSORPTION COEFFICIENT OF MANTLE FABRIC AT ROOM TEMPERATURE

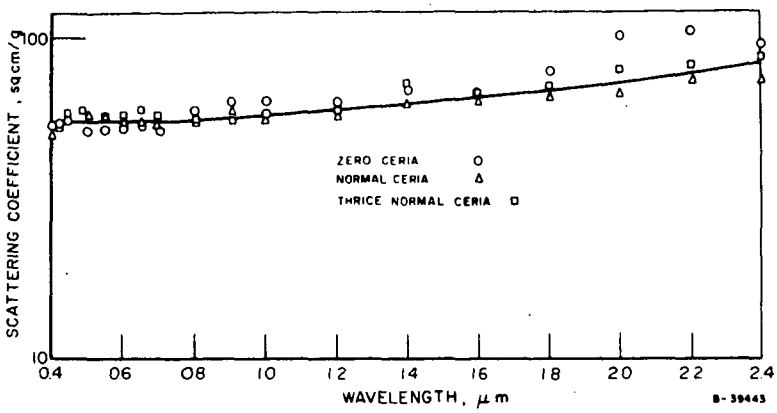

Figure 7. SCATTERING COEFFICIENT OF MANTLE FABRIC AT ROOM TEMPERATURE

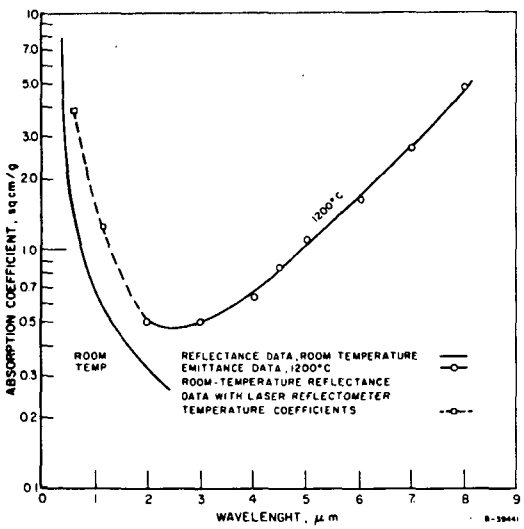

Figure 8. ABSORPTION COEFFICIENT OF MANTLE FABRIC WITH NORMAL CERIA CONTENT

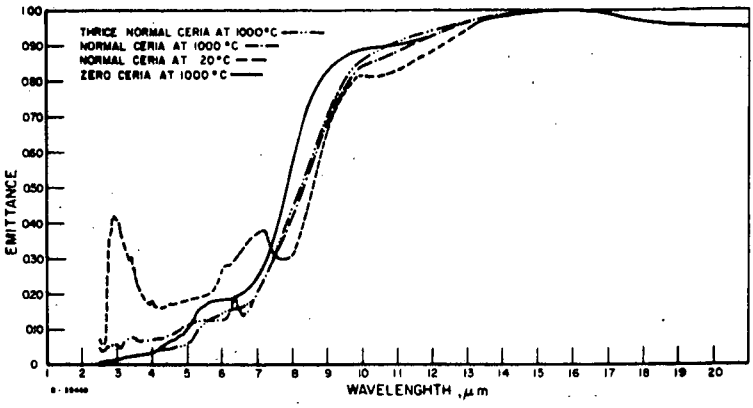

Figure 9. EMITTANCE OF GROUND MANTLE
(Obtained by Reflectance Measurement)

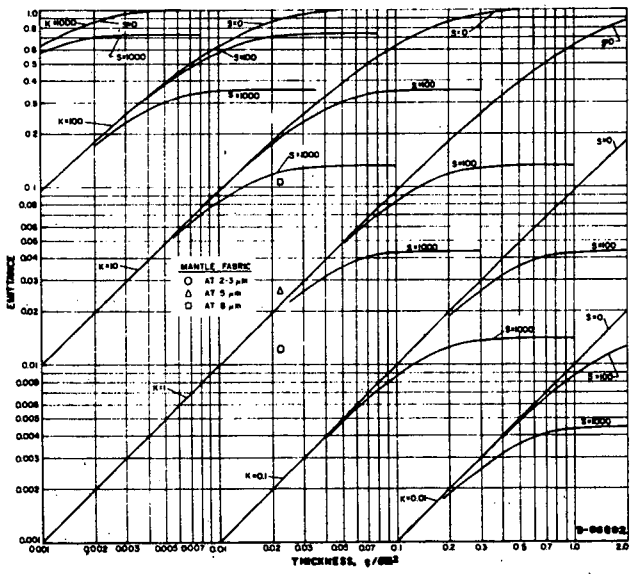

Figure 10. EFFECT OF THICKNESS; ABSORPTION COEFFICIENT, K;
AND SCATTERING COEFFICIENT, S, ON EMITTANCE
OF A DISPERSED DIELECTRIC